EUROPEAN LABORATORY FOR PARTICLE PHYSICS (CERN)

CERN-EP/98-187
30 November 1998

Analysis of Transverse Momentum Correlations in Hadronic Z Decays

The ALEPH Collaboration

Abstract

In a recent paper, evidence was presented for a significant, positive correlation between the total transverse momenta of particles on opposite hemispheres of hadronic events. A new, model independent analysis of the data has been made. Two components can be distinguished in the correlation, and quantitative estimates of each are given. The results form a significant test of Monte Carlo models and some of the physics behind them.

Submitted to Physics Letters B

The ALEPH Collaboration

R. Barate, D. Buskulic, D. Decamp, P. Ghez, C. Goy, J.-P. Lees, A. Lucotte, E. Merle, M.-N. Minard, J.-Y. Nief, P. Perrodo, B. Pietrzyk

Laboratoire de Physique des Particules (LAPP), IN^{2}P^3-CNRS, F-74019 Annecy-le-Vieux Cedex, France

R. Alemany, M.P. Casado, M. Chmeissani, J.M. Crespo, M. Delfino, E. Fernandez, M. Fernandez-Bosman, Ll. Garrido,[15] E. Graugès, A. Juste, M. Martinez, G. Merino, R. Miquel, Ll.M. Mir, A. Pacheco, I.C. Park, A. Pascual, I. Riu, F. Sanchez

Institut de Física d'Altes Energies, Universitat Autònoma de Barcelona, E-08193 Bellaterra (Barcelona), Spain[7]

A. Colaleo, D. Creanza, M. de Palma, G. Gelao, G. Iaselli, G. Maggi, M. Maggi, S. Nuzzo, A. Ranieri, G. Raso, F. Ruggieri, G. Selvaggi, L. Silvestris, P. Tempesta, A. Tricomi,[3] G. Zito

Dipartimento di Fisica, INFN Sezione di Bari, I-70126 Bari, Italy

X. Huang, J. Lin, Q. Ouyang, T. Wang, Y. Xie, R. Xu, S. Xue, J. Zhang, L. Zhang, W. Zhao

Institute of High-Energy Physics, Academia Sinica, Beijing, The People's Republic of China[8]

D. Abbaneo, U. Becker,[19] G. Boix,[25] M. Cattaneo, F. Cerutti, V. Ciulli, G. Dissertori, H. Drevermann, R.W. Forty, M. Frank, A.W. Halley, J.B. Hansen, J. Harvey, P. Janot, B. Jost, I. Lehraus, O. Leroy, P. Mato, A. Minten, L. Moneta,[21] A. Moutoussi, F. Ranjard, L. Rolandi, D. Rousseau, D. Schlatter, M. Schmitt,[20] O. Schneider, W. Tejessy, F. Teubert, I.R. Tomalin, E. Tournefier, H. Wachsmuth

European Laboratory for Particle Physics (CERN), CH-1211 Geneva 23, Switzerland

Z. Ajaltouni, F. Badaud, G. Chazelle, O. Deschamps, A. Falvard, C. Ferdi, P. Gay, C. Guicheney, P. Henrard, J. Jousset, B. Michel, S. Monteil, J-C. Montret, D. Pallin, P. Perret, F. Podlyski

Laboratoire de Physique Corpusculaire, Université Blaise Pascal, IN^{2}P^3-CNRS, Clermont-Ferrand, F-63177 Aubière, France

J.D. Hansen, J.R. Hansen, P.H. Hansen, B.S. Nilsson, B. Rensch, A. Wäänänen

Niels Bohr Institute, DK-2100 Copenhagen, Denmark[9]

G. Daskalakis, A. Kyriakis, C. Markou, E. Simopoulou, I. Siotis, A. Vayaki

Nuclear Research Center Demokritos (NRCD), GR-15310 Attiki, Greece

A. Blondel, G. Bonneaud, J.-C. Brient, A. Rougé, M. Rumpf, M. Swynghedauw, A. Valassi,[6] M. Verderi, H. Videau

Laboratoire de Physique Nucléaire et des Hautes Energies, Ecole Polytechnique, IN^{2}P^3-CNRS, F-91128 Palaiseau Cedex, France

E. Focardi, G. Parrini, K. Zachariadou

Dipartimento di Fisica, Università di Firenze, INFN Sezione di Firenze, I-50125 Firenze, Italy

M. Corden, C. Georgiopoulos, D.E. Jaffe

Supercomputer Computations Research Institute, Florida State University, Tallahassee, FL 32306-4052, USA [13,14]

A. Antonelli, G. Bencivenni, G. Bologna,[4] F. Bossi, P. Campana, G. Capon, V. Chiarella, P. Laurelli, G. Mannocchi,[5] F. Murtas, G.P. Murtas, L. Passalacqua, M. Pepe-Altarelli[2]

Laboratori Nazionali dell'INFN (LNF-INFN), I-00044 Frascati, Italy

L. Curtis, J.G. Lynch, P. Negus, V. O'Shea, C. Raine, P. Teixeira-Dias, A.S. Thompson, E. Thomson

Department of Physics and Astronomy, University of Glasgow, Glasgow G12 8QQ,United Kingdom[10]

O. Buchmüller, S. Dhamotharan, C. Geweniger, P. Hanke, G. Hansper, V. Hepp, E.E. Kluge, A. Putzer, J. Sommer, K. Tittel, S. Werner,[19] M. Wunsch

Institut für Hochenergiephysik, Universität Heidelberg, D-69120 Heidelberg, Germany[16]

R. Beuselinck, D.M. Binnie, W. Cameron, P.J. Dornan,[2] M. Girone, S. Goodsir, E.B. Martin, N. Marinelli, J. Nash, J.K. Sedgbeer, P. Spagnolo, M.D. Williams

Department of Physics, Imperial College, London SW7 2BZ, United Kingdom[10]

V.M. Ghete, P. Girtler, E. Kneringer, D. Kuhn, G. Rudolph

Institut für Experimentalphysik, Universität Innsbruck, A-6020 Innsbruck, Austria[18]

A.P. Betteridge, C.K. Bowdery, P.G. Buck, P. Colrain, G. Crawford, A.J. Finch, F. Foster, G. Hughes, R.W.L. Jones, N.A. Robertson, M.I. Williams

Department of Physics, University of Lancaster, Lancaster LA1 4YB, United Kingdom[10]

I. Giehl, C. Hoffmann, K. Jakobs, K. Kleinknecht, G. Quast, B. Renk, E. Rohne, H.-G. Sander, P. van Gemmeren, C. Zeitnitz

Institut für Physik, Universität Mainz, D-55099 Mainz, Germany[16]

J.J. Aubert, C. Benchouk, A. Bonissent, J. Carr,[2] P. Coyle, F. Etienne, F. Motsch, P. Payre, M. Talby, M. Thulasidas

Centre de Physique des Particules, Faculté des Sciences de Luminy, IN^{2}P^3-CNRS, F-13288 Marseille, France

M. Aleppo, M. Antonelli, F. Ragusa

Dipartimento di Fisica, Università di Milano e INFN Sezione di Milano, I-20133 Milano, Italy

R. Berlich, V. Büscher, H. Dietl, G. Ganis, K. Hüttmann, G. Lütjens, C. Mannert, W. Männer, H.-G. Moser, S. Schael, R. Settles, H. Seywerd, H. Stenzel, W. Wiedenmann, G. Wolf

Max-Planck-Institut für Physik, Werner-Heisenberg-Institut, D-80805 München, Germany[16]

P. Azzurri, J. Boucrot, O. Callot, S. Chen, A. Cordier, M. Davier, L. Duflot, J.-F. Grivaz, Ph. Heusse, A. Jacholkowska, D.W. Kim,[12] F. Le Diberder, J. Lefrançois, A.-M. Lutz, M.-H. Schune, J.-J. Veillet, I. Videau,[2] D. Zerwas

Laboratoire de l'Accélérateur Linéaire, Université de Paris-Sud, IN^{2}P^3-CNRS, F-91898 Orsay Cedex, France

G. Bagliesi,[2] S. Bettarini, T. Boccali, C. Bozzi, G. Calderini, R. Dell'Orso, I. Ferrante, L. Foà,[1] A. Giassi, A. Gregorio, F. Ligabue, A. Lusiani, P.S. Marrocchesi, A. Messineo, F. Palla, G. Rizzo, G. Sanguinetti, A. Sciabà, G. Sguazzoni, R. Tenchini, C. Vannini, A. Venturi, P.G. Verdini

Dipartimento di Fisica dell'Università, INFN Sezione di Pisa, e Scuola Normale Superiore, I-56010 Pisa, Italy

G.A. Blair, J.T. Chambers, G. Cowan, M.G. Green, T. Medcalf, J.A. Strong, J.H. von Wimmersperg-Toeller

Department of Physics, Royal Holloway & Bedford New College, University of London, Surrey TW20 OEX, United Kingdom[10]

D.R. Botterill, R.W. Clifft, T.R. Edgecock, P.R. Norton, J.C. Thompson, A.E. Wright

Particle Physics Dept., Rutherford Appleton Laboratory, Chilton, Didcot, Oxon OX11 OQX, United Kingdom[10]

B. Bloch-Devaux, P. Colas, S. Emery, W. Kozanecki, E. Lançon,[2] M.-C. Lemaire, E. Locci, P. Perez, J. Rander, J.-F. Renardy, A. Roussarie, J.-P. Schuller, J. Schwindling, A. Trabelsi,[24] B. Vallage

CEA, DAPNIA/Service de Physique des Particules, CE-Saclay, F-91191 Gif-sur-Yvette Cedex, France[17]

S.N. Black, J.H. Dann, R.P. Johnson, H.Y. Kim, N. Konstantinidis, A.M. Litke, M.A. McNeil, G. Taylor
Institute for Particle Physics, University of California at Santa Cruz, Santa Cruz, CA 95064, USA[22]

C.N. Booth, S. Cartwright, F. Combley, M.S. Kelly, M. Lehto, L.F. Thompson
Department of Physics, University of Sheffield, Sheffield S3 7RH, United Kingdom[10]

K. Affholderbach, A. Böhrer, S. Brandt, C. Grupen, G. Prange, P. Saraiva, L. Smolik, F. Stephan
Fachbereich Physik, Universität Siegen, D-57068 Siegen, Germany[16]

G. Giannini, B. Gobbo
Dipartimento di Fisica, Università di Trieste e INFN Sezione di Trieste, I-34127 Trieste, Italy

J. Rothberg, S. Wasserbaech
Experimental Elementary Particle Physics, University of Washington, WA 98195 Seattle, U.S.A.

S.R. Armstrong, E. Charles, P. Elmer, D.P.S. Ferguson, Y. Gao, S. González, T.C. Greening, O.J. Hayes, H. Hu, S. Jin, P.A. McNamara III, J.M. Nachtman,[23] J. Nielsen, W. Orejudos, Y.B. Pan, Y. Saadi, I.J. Scott, J. Walsh, Sau Lan Wu, X. Wu, G. Zobernig
Department of Physics, University of Wisconsin, Madison, WI 53706, USA[11]

[1]Now at CERN, 1211 Geneva 23, Switzerland.
[2]Also at CERN, 1211 Geneva 23, Switzerland.
[3]Also at Dipartimento di Fisica, INFN, Sezione di Catania, Catania, Italy.
[4]Also Istituto di Fisica Generale, Università di Torino, Torino, Italy.
[5]Also Istituto di Cosmo-Geofisica del C.N.R., Torino, Italy.
[6]Now at LAL, Orsay
[7]Supported by CICYT, Spain.
[8]Supported by the National Science Foundation of China.
[9]Supported by the Danish Natural Science Research Council.
[10]Supported by the UK Particle Physics and Astronomy Research Council.
[11]Supported by the US Department of Energy, grant DE-FG0295-ER40896.
[12]Permanent address: Kangnung National University, Kangnung, Korea.
[13]Supported by the US Department of Energy, contract DE-FG05-92ER40742.
[14]Supported by the US Department of Energy, contract DE-FC05-85ER250000.
[15]Permanent address: Universitat de Barcelona, 08208 Barcelona, Spain.
[16]Supported by the Bundesministerium für Bildung, Wissenschaft, Forschung und Technologie, Germany.
[17]Supported by the Direction des Sciences de la Matière, C.E.A.
[18]Supported by Fonds zur Förderung der wissenschaftlichen Forschung, Austria.
[19]Now at SAP AG, D-69185 Walldorf, Germany.
[20]Now at Harvard University, Cambridge, MA 02138, U.S.A.
[21]Now at University of Geneva, 1211 Geneva 4, Switzerland.
[22]Supported by the US Department of Energy, grant DE-FG03-92ER40689.
[23]Now at University of California at Los Angeles (UCLA), Los Angeles, CA 90024, U.S.A.
[24]Now at Département de Physique, Faculté des Sciences de Tunis, 1060 Le Belvédère, Tunisia.
[25]Supported by the Commission of the European Communities, contract ERBFMBICT982894.

1 Introduction

Since hadronic decays of the Z include different quark flavour pairs and must conserve total energy, some correlation between the opposite hemispheres of an event is to be expected. However neither of these mechanisms could account for the transverse momentum correlations reported in a recent paper [1]. The hadrons were produced in the reaction $e^+e^- \to Z \to$ hadrons at LEP. The analysis and interpretation of the data relied heavily on comparisons with Monte Carlo models, in terms of which it was concluded that both non-perturbative and perturbative effects were contributing to the correlation.

A new, model independent analysis of the data has been made. It shows that two components, referred to as 'soft' and 'hard', can be distinguished in the correlation. Quantitative estimates of each are given. The results test Monte Carlo models and some of the physics that lies behind them.

Given an event axis, particles are allocated to hemispheres according to the sign of the momentum component along that axis. Two different forms of thrust axes are used; precise definitions are given later. The transverse momentum for each hemisphere is defined by

$$P_t = \sum_{\text{hemisphere}} |p_{ti}| \tag{1}$$

where p_{ti} is the momentum component of the i^{th} particle transverse to the axis formed by the vector sum of all the particles, charged and neutral, in that half. An event is described by (P_{t1}, P_{t2}); the allocation to sides 1 and 2 is made at random. The correlation coefficient is

$$C(P_{t1}, P_{t2}) = \frac{\langle P_{t1} P_{t2} \rangle - \langle P_{t1} \rangle \langle P_{t2} \rangle}{\sigma_{P_{t1}} \sigma_{P_{t2}}} \tag{2}$$

where the angular brackets signify averages over the data set and σ_{P_t} is the standard deviation of the P_t distribution.

The method combines correlation with clustering based on the Durham clustering algorithm [2]. The controlling parameter in this algorithm is y_{cut}, $y_{ij} < y_{\text{cut}}$, whereby y_{ij} between two particles or clusters i, j is defined as

$$y_{ij} = \frac{2 \min\{E_i^2, E_j^2\}(1 - \cos\theta_{ij})}{E_{\text{vis}}^2}, \tag{3}$$

E_i and E_j are the respective energies of, and θ_{ij} is the angle between, the two particles and E_{vis} is the measured total energy. Such pairs are combined in sequence up to the value y_{cut}, the two four-momenta being added. The clustering algorithm is always applied to the event as a whole, and *not* to each half separately. To help the physics interpretation, it is convenient to work in terms of a parameter $m_y = \sqrt{y_{\text{cut}}\, s}$ where $\sqrt{s}$ is the known initial energy of 91.2GeV. The event axis is maintained as clustering proceeds and Eq. (1) is generalized to the cluster momenta, hence giving $P_t(m_y)$. All this is unchanged from Ref. [1].

The technique used in [1] was firstly to partition the event with respect to the thrust axis and apply a cut $P_{t1}, P_{t,2} < P_{t,\max} = 25\text{GeV/c}$ which greatly reduced the effects of total energy and momentum conservation. Discrimination between different models was then achieved by

examining the behaviour of the correlation with m_y, i.e. $C(P_{t1}(m_y), P_{t2}(m_y))$, written as $C(m_y)$. The underlying idea was that any correlation arising through soft particles (e.g. from string fragmentation [3]) would be largely removed by clustering to an appropriate value of m_y.

The present analysis is based on data acquired with the ALEPH detector in 1994 ([1] used 1992 data). The detector [4] and its performance [5] are described in detail elsewhere. As before, candidate hadron events are required to have at least 5 charged tracks with polar angle θ to the beam axis such that $|\cos\theta|$ is less than 0.95, the tracks must originate from within a cylinder of length 20 cm and radius 2 cm coaxial with the beam and centred at the nominal collision point and there are at least four hits in the principal tracking chamber, the Time Projection Chamber. The total visible energy of all such tracks must exceed 10% of the total centre of mass energy.

For the final data set, charged and neutral particles are reconstructed as 'energy flow objects' [5] and events with total energy less than 70GeV are rejected. The selected event axis is required to lie within the range of polar angles from 35 to 145° of the beam axis. Any surviving τ pairs are removed by requiring that at least one side has $P_t > 2.0$GeV/c. More details on the event selection and analysis can be found in [1]. About 1.2 million events remain after these cuts.

2 Low $\mathbf{m_y}$ correlation

The study of correlations at low m_y is based on changes in C with m_y. As clustering proceeds, sometimes a cluster will form near 90° to the event axis, such that only a small modification to the event would be needed for the entire cluster to appear on the other side. When viewed from one side, this effect, for a set of events, can be seen in terms of fluctuations about average behaviours; it is a form of 'shot noise' akin to that experienced with statistical fluctuations in electric currents. However, viewed from an event as a whole, such a cluster will not only raise P_t by an amount δ on one side but also lower P_t by a comparable amount on the other. The important point is that, irrespective of the sign of δ, such shot noise fluctuations will always make a negative contribution to the correlation; in the simplest case, assuming δ to be uncorrelated with either P_t and $\overline{\delta} = 0$, by $-\overline{\delta^2}/(\sigma_{P_{t1}}\sigma_{P_{t2}})$. The effect can be of particular importance for the present study, in which m_y is varied over a wide range and an individual cluster formed at higher m_y can consequently carry a high value of transverse momentum. The new analysis attempts to circumvent this shot noise contribution. Two approaches are described.

2.1 $\mathbf{P_t(m_y)}$ on one side only

Events are partitioned with respect to the thrust axis. The selection $P_{t1}, P_{t2} < P_{t,\max} = 25$GeV/c is imposed. Events are clustered as described above but, rather than P_{t1} and P_{t2} being measured at the same m_y, the correlation is examined between $P_{t1}(m_y)$ and $P_{t2}(m_y = 0)$. As always sides 1 and 2 are chosen at random. In the example above, side 1 will sometimes lose P_t to, sometimes gain P_t from, side 2, but there will no longer be a term corresponding to $-\delta^2$ since the number representing P_{t2} does not change - the δ is on one side only. More generally, in the sum over events $\sum P_{t1}(m_y)\, P_{t2}(0)$ needed for the correlation, Eq. (2), event-to-event *fluctuations* in the

transfer of P_t will be averaged out, while still leaving open a possible dependence of either P_t on the other. This correlation is written as $C(m_y, 0)$, meaning that P_{t1} is taken at the given m_y, P_{t2} at $m_y = 0$.

Figure 1(a) shows the uncorrected data; corrections for detector effects will be discussed below. There is a relatively rapid fall in $C(m_y, 0)$ from 0.079 at $m_y = 0$ to a low of 0.050 at about $m_y = 6$GeV followed by a slow rise to 0.055 at $m_y = 15$GeV. Because it occurs at low m_y, below 5GeV, this fall is referred to as the 'soft correlation'. As an indication of its width, half the fall occurs within $m_y \approx 1.4$GeV.

2.2 Event groups

While the $C(m_y, 0)$ correlation is designed to remove the shot noise effect, it does so at the expense of only having clustered the softer particles from one hemisphere. The second technique for reducing the effect of fluctuations is to follow the average behaviour with m_y of groups of events characterized by having nearly the same initial (P_{t1}, P_{t2}) values. The individual P_t values are now measured after clustering from both hemispheres, thus enhancing the correlation.

Prior to clustering, the set of events with $P_{t1},\ P_{t2} \leq P_{t,\max} = 25$GeV/c is subdivided into 1GeV/c square cells (k, l), $1 \leq k \leq 25; 1 \leq l \leq 25$, so 625 in all. Each event contributes twice; once to (k, l), once to (l, k), to give $n_{kl} = n_{lk}$ members in a cell. Letting A_{kl} be the average value of P_{t1} for the events in cell (k, l), a correlation can be found as in Eq. (2) from the substitution:

$$\langle P_t \rangle \longrightarrow \frac{1}{N} \sum_{k,l} n_{kl} A_{kl} \qquad \langle P_{t1} P_{t2} \rangle \longrightarrow \frac{1}{N} \sum_{k,l} n_{kl} A_{kl} A_{lk} \qquad N = \sum_{k,l} n_{kl} \tag{4}$$

To calculate the standard deviation, the r.m.s. value of P_t at each cell, referred to as B_{kl}, is also needed. The cell size chosen is sufficiently small for the use of these averages in place of Eq. (2) to have a negligible effect on the calculated correlation at $m_y = 0$. So far all that has been done is to digitize the initial P_t values.

The events are now clustered to some given m_y. Following the group in a particular cell (k, l), P_t values after clustering will generally span a wide range of values (usually lower). For example, the same initial P_{t1} might represent in one case a half event with a single, central core and low momentum particles at larger angles; P_{t1} in this case would probably fall to zero (i.e. a single cluster) quite quickly. In another, the half event might initially produce two clusters which only finally coalesced to one at an appreciably higher m_y. Sometimes clustering will move P_t from side 2 to side 1; sometimes the other way. Given sufficient events in each cell, e.g. > 100, these fluctuations will tend to average out. New averages $A_{kl}(m_y)$, also $B_{kl}(m_y)$, are therefore determined for each cell and the overall correlation is recalculated as in (4). This averaging still preserves the underlying correlation; if, for example, higher P_{t2} is associated with higher P_{t1}, this will still show in the averages. This correlation is referred to as $\overline{C}(m_y)$.

The results for $\overline{C}(m_y)$ are also shown on Fig. 1(a) where they can be directly compared with $C(m_y, 0)$. The data show a generally similar behaviour; the fall has more of a tail, but reaches a near constant value of $\overline{C}$ above about $m_y = 6$GeV, $y_{\rm cut} = 0.0043$. The two values agree at $m_y = 0$, showing that the digitization of P_t has a negligible effect on the correlation. Half of the

fall has occurred by $m_y \approx 1.55$GeV, similar therefore to the 1.4GeV observed with $C(m_y, 0)$. More details for both correlations are given in Table 1, where the 'plateau' level is taken as the average of values at 6, 8, 10 and 12GeV, and the soft correlation is the value of $C(m_y = 0)$ relative to this plateau. The choice of 1GeV/c for the cell size in $\overline{C}(m_y)$ is not critical; doubling or halving this size changes these numbers by less than 0.0003. The fall in $\overline{C}(m_y)$ is about twice that seen in $C(m_y, 0)$. It is even larger for $C(m_y)$ analysed in [1]. $C(m_y)$ is equivalent to a $\overline{C}(m_y)$ in which the cell size used for averaging goes to zero. Comparing $C(m_y)$ with $\overline{C}(m_y)$ and then $C(m_y, 0)$, one sees a clear tendency for the reduction of the shot noise fluctuations which were making a major contribution to the correlation.

Axis, correlation	$C(m_y = 0)$	Range (GeV)	Plateau	Soft correlation
Thrust, $C(m_y, 0)$	0.079	6–12	0.051	0.028 ± 0.001
Thrust, $\overline{C}(m_y)$	0.079	6–12	0.022	0.057 ± 0.001
Thrust, $C(m_y)$	0.079	6–12	-0.021	0.100 ± 0.001

Table 1. Magnitudes of the soft correlation for data (uncorrected for detector effects). Events are partitioned with respect to the thrust axis. Errors are statistical only.

2.3 The cluster axis

At a sufficiently high m_y, all events reduce to two clusters. When this occurs, the two halves of an event have 3-momenta $\mathbf{P_1}$ and $\mathbf{P_2}$, and a 'cluster axis' is defined along the vector difference $\mathbf{P_1} - \mathbf{P_2}$. In effect, one is clustering first, then finding the thrust axis, rather than the other way round. For most events the partitioning is unaltered; differences can arise with complex events containing e.g. four jets which could have 2 jets on each side using the thrust axis and 1 plus 3 using the cluster axis. For an analysis over a wide range of m_y it is interesting to partition the event through a reconstruction of the inferred, initial $q\bar{q}$ rather than from the final hadrons.

The previous analyses were therefore repeated with the events partitioned by the cluster axis. Figure 1(b) shows the results, on the same scale as Fig. 1(a). The dotted line again indicates $C(m_y)$. Comparing the two figures, the immediate effect of using the cluster axis is to move the correlations in a negative direction, e.g. $\overline{C}(m_y)$ is now close to zero at high m_y. The magnitudes of the soft correlations are extracted as for Table 1 and are shown in Table 2. They are very close to the values using the thrust axis given in Table 1. The values of m_y at which half the falls have occurred are also unchanged.

Axis, correlation	$C(m_y = 0)$	Range (GeV)	Plateau	Soft correlation
Cluster, $C(m_y, 0)$	0.053	6–12	0.025	0.028 ± 0.001
Cluster, $\overline{C}(m_y)$	0.053	6–12	-0.006	0.059 ± 0.001

Table 2. Similar to Table 1 but with the events partitioned with respect to the cluster axis. Errors are statistical only.

2.4 The magnitude of the soft correlation

The general pattern and stability of the soft correlation encourages an attempt to measure this quantity, written as $C_{\rm soft}$. Attention is concentrated on the cluster axis measurement of $\overline{C}(m_y)$ in Fig. 1(b), partly because the effect to be measured is larger with $\overline{C}(m_y)$, thereby reducing sensitivity to other possible contributions, in particular any assumption about the soft correlation from side 1 to 2 in $C(m_y, 0)$; partly because, with the cluster axis, the correlation above the soft region is seen to be small, and therefore less is assumed in projecting it back to $m_y = 0$.

If the value of $C_{\rm soft}$ is to be meaningful, it should not be sensitive to the exact values of the cuts used to define the data set. That this is the case is shown in Table 3 where the measurements (uncorrected) of $\overline{C}(m_y)$ given in Table 2 are repeated, varying in turn the total energy and polar angle cuts. Changes here are small, < 0.001. The fourth row shows what happens if y_{ij} and m_y in (3) are calculated in terms of $\sqrt{s} = 91.2$GeV rather than in terms of $E_{\rm vis}$, there being a possibility that event to event fluctuations in $E_{\rm vis}$ could introduce an extraneous correlation. The value at $m_y = 0$ is, of course, unaffected; the plateau level rises by about 0.0017. This is considered as an uncertainty rather than as a correction. The fifth row shows the sensitivity to the $P_{t,\rm max}$ cut. This is a rather different test as the data set itself is different; there is no fundamental reason why the measured soft correlation between the two sides should not vary with the range of P_t used. Nevertheless, the change in $C_{\rm soft}$ is still relatively small.

Cuts	$C(m_y = 0)$	Plateau	$C_{\rm soft}$
From Table 2	0.0530	-0.0061	0.0591 ± 0.0011
Vary total energy (70GeV) $65 \rightarrow 75$GeV	$0.0538 - 0.0527$	$-0.0063 - -0.0056$	$0.0601 - 0.0583$
Vary $\theta(35 - 145^\circ)30 - 150^\circ \rightarrow 40 - 140^\circ$	$0.0528 - 0.0536$	$-0.0065 - -0.0058$	$0.0593 - 0.0594$
Fixed energy for m_y	0.0530	-0.0044	0.0574
Vary $P_{t,\rm max}(25\text{GeV/c})20 \rightarrow 30$GeV/c	$0.0575 - 0.0464$	$0.0011 - -0.0128$	$0.0564 - 0.0592$

Table 3. Sensitivity of $C_{\rm soft}$ as measured to variations in the cuts on total energy and polar angle, the definition of m_y and $P_{t,\rm max}$ of the data set. The left hand column shows, in brackets, the standard values, followed by those used in the test. The right hand columns show the resulting values, e.g. dropping the total energy cut from the standard 70GeV to 65GeV changes $C_{\rm soft}$ from 0.0591 to 0.0601 (values are given to 4 decimal places in order to show the *changes* in $C_{\rm soft}$).

Estimates of the corrections for detector effects are given in Table 4. They are made by running the same analysis program, including the $P_{t,\rm max}$ cut of 25GeV/c, on generated and reconstructed Monte Carlo events, noting the change $C_{\rm gen} - C_{\rm rec}$ at each m_y point, adding this to the measured data point and hence calculating the change $\Delta C_{\rm soft}$ in $C_{\rm soft}$. Detailed comparisons with several generators will be made in section 4. Since JETSET, for which the largest sample of such events is available, does not give a good, overall description of the data, lacking a plateau region at higher m_y, $C_{\rm soft}$ is taken as $C(0) - \overline{C}(m_y = 6)$. A modification, 'culled JETSET', will be described in section 5, where it is shown that the disagreement is largely the result of a relative excess of JETSET events having P_t high on one side, low on the other. These can be removed from the events as generated; the estimate for $\Delta C_{\rm soft}$ is almost unchanged. HERWIG gives a similar result, though with a higher statistical error. Although the general agreement here is encouraging, considerable uncertainty attaches to just how reliable is this correction. A corresponding analysis of the 1992 data and JETSET simulation gave

an uncorrected value of 0.0605±0.0016, close therefore to the 1994 measurement, whereas the indicated correction from JETSET was only 0.0034. Significant improvements had been made to the simulation, and the 1994 value is therefore preferred. In the circumstances it is proposed to add 0.010 ± 0.006 to the uncorrected value. Since other effects are all small, this gives a result of $C_{\rm soft} = 0.069 \pm 0.006$. Finally, JETSET is used to compare events including, and without, initial state radiation. Changes are small, less than 0.0005 in $C_{\rm soft}$, and can be neglected.

Data set	$C(m_y = 0)$	$\overline{C}(m_y = 6)$	$C_{\rm soft}$	$\Delta C_{\rm soft}$
ALEPH			0.0591 ± 0.0011	
JETSET gen.	0.0395	−0.0231	0.0626 ± 0.002	
JETSET rec.	0.0269	−0.0264	0.0533 ± 0.002	0.0093
JETSET gen, culled.	0.0574	−0.0077	0.0651 ± 0.002	
JETSET rec, culled.	0.0438	−0.0102	0.0540 ± 0.002	0.0111
HERWIG gen.	0.0781	−0.0029	0.0810 ± 0.004	
HERWIG rec.	0.0628	−0.0067	0.0695 ± 0.004	0.0115

Table 4. Values of $C_{\rm soft}$ for Monte Carlo generators, used to estimate detector effects (values are given to 4 decimal places to show the *changes* in $C_{\rm soft}$). The Table can also be used to compare JETSET and HERWIG values of $C_{\rm soft}$ with the ALEPH measurement.

3 The region above $m_y = 6$GeV

From the preceding analysis, and as can be seen directly from Fig. 1(a,b), one can examine the correlations after removing the soft coupling if the events are first clustered to $m_y \geq 6$GeV, a region referred to here as the 'hard correlation' or 'hard' region of m_y.

Neither $C(m_y, 0)$ nor $\overline{C}(m_y)$ is appropriate for a study of the hard region: the $P_{t,\rm max}$ cut is applied to the hadrons, $C(m_y, 0)$ leaves one side unclustered, $\overline{C}(m_y)$ is better but is still based on cells defined by the hadrons. In fact, $C(m_y, 0)$ and $\overline{C}(m_y)$ are best suited to measuring changes in the correlations at low m_y. For a consistent examination of the hard correlation, all the analysis should be based on the events after pre-clustering. As a corollary, the cluster axis rather than the thrust axis is used to partition the events.

3.1 $\mathbf{C_{tot}(m_y)}$, the full data set

The simplest and most direct measurement that fulfils the above pre-clustering condition is to determine the P_t correlation as a function of m_y, that is $C_{\rm tot}(P_{t1}(m_y), P_{t2}(m_y))$, or more briefly $C_{\rm tot}(m_y)$, where $C_{\rm tot}$ implies that the entire data set has been used, i.e. there is no $P_{t,\rm max}$ cut. The result is shown in Fig. 1(c) for a series of values of m_y from 50GeV down to zero.

The behaviour of $C_{\rm tot}$ at very high m_y is of interest, as in a sense it gives information about the events at very early times. For example, the dashed curve shows the predicted $C_{\rm tot}(m_y)$, using the JETSET $O(\alpha_s^2)$ matrix element [6] ($\Lambda_{QCD} = 0.123$, $y' = 1.0$), for $d\bar{d}$ partons. In this

region the great majority of events have just two clusters; a small fraction have three and there are none with four. Two cluster events have P_t values (0,0); 3 cluster correspond to $(0, \text{high})$ or $(\text{high}, 0)$. If these have relative weights 1, f, f, and for simplicity we assume a fixed, single high P_t value, then

$$C_{\rm tot} = \frac{-f}{1+f}$$

and $C_{\rm tot}$ is essentially equivalent to f. $C_{\rm tot}$ must therefore be negative at high m_y, tending to a limit of zero as f approaches zero. At somewhat lower m_y the correlation will be sensitive to the 4 cluster events and how these divide between $2-2$ and $1-3$.

There is relatively little variation in $C_{\rm tot}$ from $m_y = 12$ down to 6GeV. An overall measure of the hard correlation can therefore conveniently be obtained by noting the magnitude of $C_{\rm tot}$ at the minimum. Since $C_{\rm tot}$ only depends on clustering, and of course the use of P_t, the near independence of m_y should be useful for making comparisons with Monte Carlo models, also possibly with theory. For ALEPH the (uncorrected) minimum value is -0.0524 ± 0.0010, at about $m_y = 9$GeV and therefore safely above the soft region.

While the main concern here is with the behavour above 6GeV, Fig. 1(c) by itself illustrates nicely the very different behaviour in the two regions. In model terms one can almost picture the evolution of the $q\bar{q}$ with decreasing m_y; the gradual emergence of a parton branching structure, terminating in the final fragmentation. Equally, starting from $m_y = 0$, one can also see how effectively pre-clustering to $m_y = 6$GeV removes the soft correlation.

The stability of the minimum value has been investigated. Making the same changes to total energy and polar angle cuts as in Table 3 alters $C_{\rm tot}$ by less than 0.0005. Unlike $C_{\rm soft}$, there is no $P_{t,\rm max}$ cut, which must also help. Using the alternative, $\sqrt{s}$ based, definition of m_y changed the ALEPH value from -0.0524 to -0.0507, again considered as an uncertainty. However, as one might suspect from Figs. 1(a,b), the use of the hadron-based thrust axis has a major effect, raising the minimum to -0.043 ± 0.0010. It is therefore important in this case to specify that the cluster axis is used to partition the events.

Reconstruction errors are smaller than for $C_{\rm soft}$. Making the same tests as described in Table 4, the average of the three corrections adds 0.0025 to the measured -0.0531, making -0.0506. There was no significant contribution from initial state radiation. Because of general uncertainties in the correction procedure, it is proposed to assign a systematic error of ± 0.003 to the corrected value. Since statistical errors are again small, this gives a value for minimum $C_{\rm tot}$ using the cluster axis of -0.051 ± 0.003.

3.2 The $\mathbf{P_{t,max}}$ cut in the hard region

While $C_{\rm tot}(m_y)$, the correlation for the entire data set as a function of m_y, is conceptually simple, total energy conservation manifestly plays an important role. The earlier paper [1] started with the observed correlation as a function of the cut $P_{t,\rm max}$. By reducing $P_{t,\rm max}$ to 25GeV/c, the very asymmetric events were removed, giving a subset of events for which any correlation contribution from total energy conservation should be small. In this section, a similar $P_{t,\rm max}$ cut is applied after pre-clustering the events, i.e. as the soft coupling is progressively removed,

thereby exposing any residual hard correlation. For the technique to be applied, minimum $P_{t,\max}$ must be appreciably above m_y. The resulting family of correlations will be denoted by $C_{m_y}(P_{t,\max})$, where m_y refers here to the level of pre-clustering.

Events are pre-clustered at a sequence of m_y values: 0, 1, 2 to 6GeV, and are partitioned with respect to the cluster axis. Plots are made of $C_{m_y}(P_{t,\max})$, i.e. of $C(P_{t1}(m_y), P_{t2}(m_y))$ where $P_{t1}, P_{t2} \leq P_{t,\max}$ at the corresponding m_y. The results are shown in Fig. 1(d). There is a general tendency for only a small variation in C with $P_{t,\max}$ between 25 and 12.5GeV/c at all m_y, including $m_y = 5$ and 6GeV, where soft contributions should have vanished. As in [1] this is in line with the idea that the (negative) contribution from energy conservation becomes small as events with very high P_t are removed. The plots come together quite strikingly at $m_y = 4$, 5, 6GeV over all $P_{t,\max}$, evidence of how pre-clustering removes the soft correlation. The residual correlation is estimated by taking the average value of $C_{m_y}(P_{t,\max})$ at $m_y = 6$GeV, $P_{t,\max} =$ 15, 20 and 25GeV/c, giving about -0.013. The results are again found to be insensitive to the changes previously described in the total energy cut; the polar angle cut; the use of fixed $\sqrt{s}$ in m_y and initial state radiation. Making the same corrections for detector effects as described in Table 4 gave corrections ranging from +0.0014 to +0.0037. The figures therefore indicate a small, residual correlation of about -1%.

4 Comparisons with Monte Carlo generators

It is interesting to compare the results with those from Monte Carlo generators, not only to test the generators, but also for some of the underlying physics. The presence of both hard and soft contributions was inferred in [1] from detailed comparisons with the partonic and fragmentation phases of JETSET and ARIADNE, whereas the analysis presented here distinguishes two regions of m_y, and the corresponding correlations, directly from the data.

A large sample of Monte Carlo events was generated using the program JETSET 7.4 [6] modified to include detailed information on heavy flavour decays. These events were passed through a detailed simulation of the detector and analysed as for the ALEPH data. A similar but smaller sample of HERWIG version 5.6 [7] was generated and analysed. Comparisons are also made with hadron events generated with ARIADNE 4.04 [8]. All these generators had been tuned to ALEPH data [9]. Finally, ARIADNE was independently used to generate parton showers from an initial $d\bar{d}$ state in which the shower cut-off parameter $p_{\perp,\min}$ was reduced to 0.3GeV/c. It had already been noted [1] that the correlation $C(m_y = 0)$ for these partons was close to that found in the ALEPH data, also that there was some support for using ARIADNE to extrapolate beyond $O(\alpha_s^2)$ [1, 10]. Since hadrons are observed, such a correlation also relies on, and ultimately might help to test, the concept of local parton hadron duality [11], LPHD, which is therefore used to denote the correlations using ARIADNE partons.

The generators are tested against the four main correlations: $C(m_y, 0)$; $\overline{C}(m_y)$; $C_{\rm tot}(m_y)$; and $C_{m_y}(P_{t,\max})$, Fig. 2(a) to (d) respectively. The first two mainly concern, and are sensitive to, behaviour in the soft region, the last two mainly the hard m_y region. The measured ALEPH values are corrected by adding, on a point by point basis, the change $(C_{\rm gen} - C_{\rm rec})$ in the corresponding values for the JETSET data set described above. Figure 2 includes these values before and after correction. The corrections are greatest in the soft region, attaining a maximum

value of +0.012 at $m_y = 0$, but are small at higher m_y.

It is evident that P_t correlations can be a severe test of a Monte Carlo simulation. While JETSET describes quite well the variation with m_y in the soft region and also the magnitude of $C_{\rm soft}$ (see Table 4), it fails in the hard region, seen most strikingly in Fig. 2(c). Evidence will be presented in section 5 that an excess of events with high P_t on one side, low on the other, is responsible.

ARIADNE hadrons badly overestimate the magnitude of the correlation at $m_y = 0$. This persists throughout the m_y range. The possibility of a perturbative explanation of the Lund string effect [3], often referred to as the drag effect [12], has been raised. The drag effect results from colour coherence in which colour conservation leads to gluon radiation from boosted $q\bar{q}$ dipoles. These gluons tend to populate the same angular regions as those identified by the string. The correlation in the ARIADNE generator arises both in the parton cascade, itself described in terms of boosted dipoles, and, as in JETSET, in the string. The excess correlation could therefore indicate a certain level of overlap, or double counting, between the two explanations. Since ARIADNE fails to give any plateau, or even minimum value for $\overline{C}(m_y)$, Fig. 2(b), it is not possible to give a meaningful ARIADNE value for $C_{\rm soft}$.

The result for the ARIADNE parton model, LPHD in Fig. 2, gives the best agreement for the total correlation $C_{\rm tot}$ in the hard correlation region of Fig. 2(c). But examination of especially Fig. 2(b) shows the absence of any sort of plateau region; although the correlation at $m_y = 0$ is comparable with the ALEPH result, the fall off in $\overline{C}$ with m_y is much too slow and again it is not possible to separate the hard and soft regions. The comparison with JETSET, which does give a good description of the variation with m_y at low m_y, may indicate a possible basis for distinguishing the string and drag mechanisms for particle flow [12].

Of the four generators discussed, HERWIG clearly gives the best overall description. It does describe well the behaviour in the soft region (though from Table 4 $C_{\rm soft}$ itself is a little high) and does tend to flatten out at higher m_y, Fig. 2(a,b). It is the only generator to give a good description of the residual hard correlation, Fig. 2(d).

5 JETSET and the perturbative structure of events

In this section it is shown how clustering ideas, combined with partition, can be developed to analyze the structure of events in the hard region, and hence expose where the JETSET events, as generated, are failing. An empirical correction that brings these events much closer to the ALEPH data on correlations, is described.

Events are clustered in steps of $m_y = 5$GeV, starting with step 1 to correspond to the hadrons; step 2 to $m_y = 5$GeV and so on up to step 11, $m_y = 50$GeV. At some stage in the clustering, the tracks in a hemisphere will collapse to a single cluster (i.e. with $P_t = 0$). The steps at which this happens are described by two integers (i, j), $1 \leq i \leq j \leq 12$ where the first side to do so collapses at step i, the second at step j. Thus if one such collapse occurs at say 17GeV, i.e. at step 5, and the other at say 7GeV, i.e. at step 3, the event is categorized as (3,5).

Events are accumulated in an array i, j with N_{ij} members. The numbers N_{ij} describe the hard structure of events in considerable detail. From a comparison of the ALEPH and reconstructed JETSET arrays, the greatest differences are found for $i \leq 2$, i.e. events in which one side has collapsed to a single cluster by $m_y = 5$GeV. The ratio of JETSET to ALEPH events signals a relative excess of such events which increases approximately linearly with j from about 4% at $j = 2$ to about 24% at $j = 11$.

The excess fraction of JETSET events can be rejected. This is interesting for several reasons. Firstly, as a model of QCD processes and hadronization JETSET is recognized as giving a good description of data over a wide range of reactions [13]; so when, as here, it fails quite badly, it is important to know more. Secondly, JETSET is used in the present paper to estimate corrections for detector effects; the presence of an excess negative correlation might be significant. Thirdly, in the present study, JETSET gives quite a good description of $C_{\rm soft}$; is this affected by its failure in the hard region?

The JETSET data set was re-analyzed with the estimated excess of JETSET events, as described by the linear relationship above, removed or 'culled'. The cull is applied at the generator level. It would be more direct to apply the cull on reconstructed events, but this could distort the use of the resulting data set in exploring corrections for detector effects. Though only a 'first order' correction, the correlations determined with the culled JETSET are in much better agreement with ALEPH. Figure 3(a) and 3(b) show the new comparison with ALEPH data for $C(m_y, 0)$ and $\overline{C}(m_y)$, to be compared with the unculled JETSET of Figs. 2(a) and 2(b) respectively. The JETSET points are still a little low, but are much closer to ALEPH and in particular the behaviour in the soft region is very well described. From Table 4, the value of $C_{\rm soft}$ at generator level is increased by only 0.0025 by the cull, though this is complicated by the difference in the 'background' shapes in the two cases. In the hard region, the correlation $C_{\rm tot}(m_y)$ is now much closer to the data than in Fig. 3(c). Lastly, C_{m_y} as a function of $P_{t,\rm max}$ *after* the events have been clustered at $m_y = 5$GeV (also 0 and 2GeV), can be compared with Fig. 3(d). Though again JETSET distributions are a little low, they do now clearly show a similar structure to that seen in the data.

6 Summary and Conclusions

Correlations are formed between quantities P_{t1}, P_{t2}, the total, internal transverse momenta within the two hemispheres of hadronic events from Z decay. They are examined as a function of a clustering parameter $m_y = \sqrt{y_{\rm cut}\ s}$ based on the Durham cluster algorithm, where $\sqrt{s}$ is the total energy. It is found advantageous to partition the events with a thrust axis determined *after* clustering each event to just two clusters.

Two correlations, $C(m_y, 0)$ and $\overline{C}(m_y)$, designed in particular to circumvent the 'shot noise' contribution, are described and applied to ALEPH data. They give a consistent picture of a soft correlation below $m_y = 6$GeV ($y_{\rm cut} = 0.0043$), which has a magnitude of $C_{\rm soft} = 0.069 \pm 0.006$ at a $P_{t,\rm max}$ of 25GeV/c and which falls to $C_{\rm soft}/2$ at $m_y \approx 1.5$GeV. The error is dominated by systematic uncertainties in event reconstruction.

The correlation for the full data set, $C_{\rm tot}(m_y)$ is examined as a function of m_y. Starting

from the highest $m_y, 50\text{GeV}$, this shows the growth in the (negative) correlation in the hard region, terminating in a rapid rise in the soft region. $C_{\text{tot}}(m_y)$ attains a minimum value of -0.051 ± 0.003 at about $m_y = 9\text{GeV}$, safely therefore above the soft region.

A fourth correlation, $C_{m_y}(P_{t,\max})$, allows detailed changes to be followed as events are pre-clustered to remove the soft coupling and an upper bound is imposed on P_t to minimize coupling from total energy conservation. With both these applied, the residual correlation is small, about -1.0%.

JETSET gives quite a good description of how the correlations vary in the soft region but fails badly in all tests at higher m_y, generally by giving too strong a (negative) correlation. ARIADNE hadrons, on the other hand, clearly give too large a positive correlation, possibly attributable to having both string and drag mechanisms in the generator. ARIADNE partons (LPHD) are generally closer to describing the data than either JETSET or ARIADNE hadrons, but fail to distinguish the soft and hard regions in $\overline{C}(m_y)$. The contrast with JETSET may indicate a possible basis for distinguishing the string and drag mechanisms for interjet particle flow [12]. HERWIG gives the best overall agreement with the data.

The clustering technique is used to analyze the failure of JETSET events at high m_y. The application of an *ad hoc* correction brings the simulation much closer to the data.

Acknowledgements

We wish to thank our colleagues in the CERN accelerator divisions for the excellent operation of the LEP collider. We also thank the engineers and technicians from all the collaborating institutions for their contributions to the success of ALEPH. Those of us from non-member states wish to thank CERN for its hospitality.

References

[1] ALEPH Collaboration, *'Transverse Momentum Correlations in Hadronic Z Decays'* Z. Phys. C 73 (1997) 421

[2] W.J.Stirling, J. Phys. G 17 (1991) 1567

[3] B.Andersson, G.Gustafson and B.Söderberg, Z. Phys. C 20 (1983) 317

[4] ALEPH Collaboration, *'ALEPH: A Detector for Electron-Positron Annihilations at LEP'* Nucl. Inst. and Meth. A294 (1990) 121

[5] ALEPH Collaboration, *'Performance of the ALEPH Detector at LEP'* Nucl. Inst. and Meth. A360 (1995) 481

[6] T.Sjöstrand, Comp. Phys. Comm. 82 (1994) 74

[7] G.Marchesini et al., Comp. Phys. Comm. 67 (1992) 465

[8] L.Lönnblad, Comp. Phys. Comm. 71 (1992) 15

[9] ALEPH Collaboration, *'Properties of Hadronic Z Decays and Tests of QCD Generators'* Z. Phys. C 55 (1992) 209

[10] B.Andersson, G.Gustafson and C.Sjögren, Nucl. Phys. B 380 (1992) 391

[11] Ya.I.Azimov et al., Phys.Lett. B 165 (1985) 147; Z. Phys. C 27 (1985) 65

[12] V.A.Khoze and W.Ochs, Int. J. Mod. Phys. A12 1997.

[13] ALEPH Collaboration, *'Studies of Quantum Chromodynamics with the ALEPH Detector'* Physics Reports 294 (1998) 1

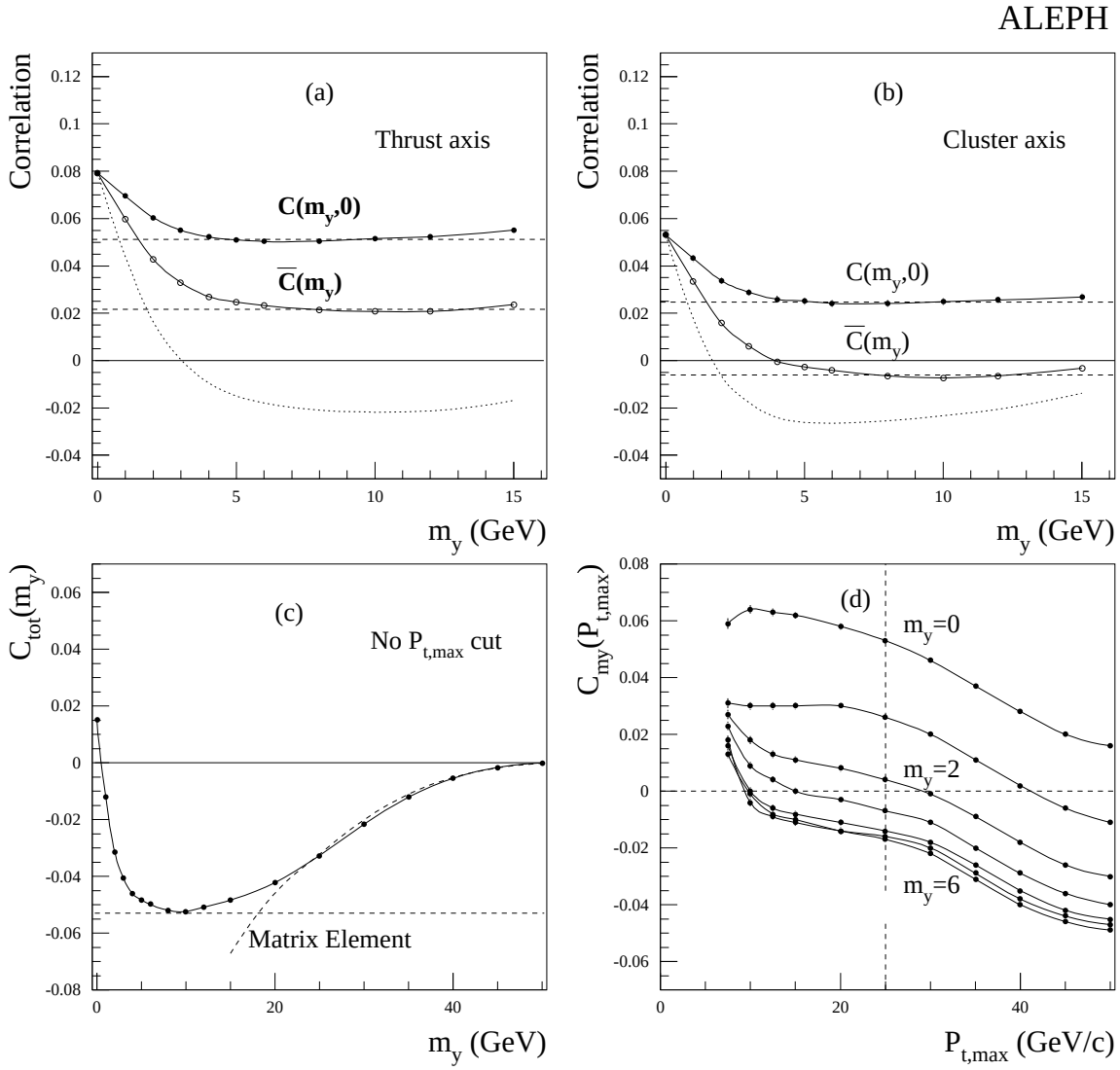

Figure 1: Correlations for ALEPH data. a) and b) $C(m_y, 0)$ and $\overline{C}(m_y)$, with events partitioned with respect to the thrust axis and cluster axis respectively. The dashed lines indicate the 'plateau' levels (Tables 1 and 2). The dotted lines show $C(m_y)$ as from [1]. c) $C_{\rm tot}(m_y)$, the correlation for the full set of events. d) $C_{m_y}(P_{t,\rm max})$, the variation of the correlation with a $P_{t,\rm max}$ cut for different levels of pre-clustering, $m_y = 0$ to 6GeV.

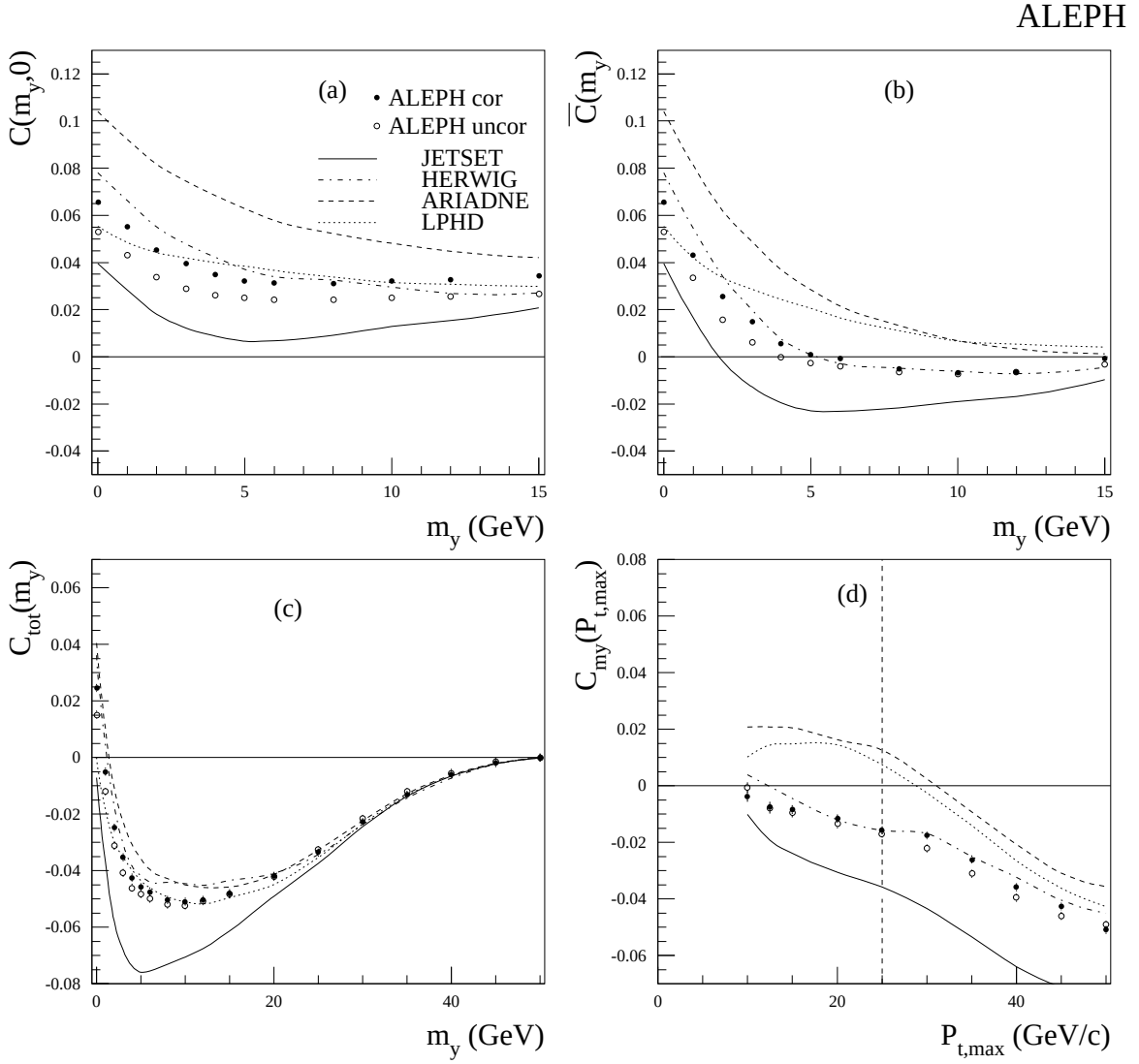

Figure 2: Four Monte Carlo generators compared with corrected ALEPH data. The ALEPH data is also shown before correction. The cluster axis is used throughout. a) and b) $C(m_y, 0)$ and $\overline{C}(m_y)$ as in Fig. 1. c) $C_{\rm tot}(m_y)$ as in Fig. 1(c). d) $C_{m_y}(P_{t,\rm max})$ at $m_y = 5$GeV. LPHD refers to a model based on ARIADNE partons.

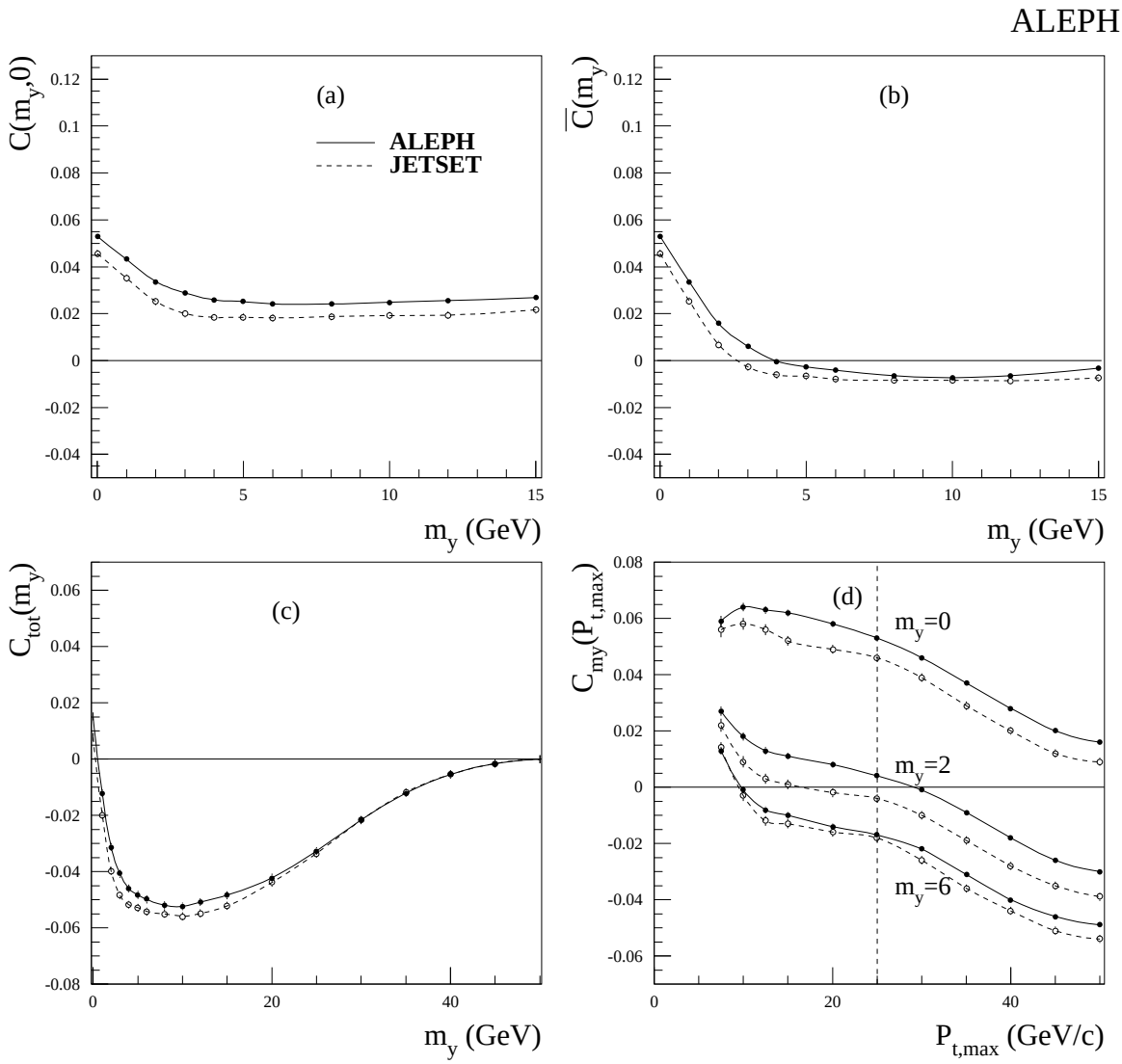

Figure 3: Behaviour of reconstructed JETSET, again compared with ALEPH, after the removal (cull) of some asymmetric events as described in the text. JETSET prior to the cull is seen in Fig. 2.